DETERMINATION OF THE ANODE VOLTAGE FALL IN TIG ARCS BY USING A MODIFIED SPLIT-ANODE DETECTOR

Louriel Oliveira Vilarinho
Laboratory for Welding Process Development – LAPROSOLDA, Federal University of Uberlândia - UFU, Campus Santa Mônica, 38400-902, MG, Brazil, e-mail vilarinho@mecanica.ufu.br.

Carlo Fanara
SIMS, WERC, Cranfield University, Wharley End, Cranfield, Bedfordshire MK43 0AL, UK, e-mail c.fanara@cranfield.ac.uk

Américo Scotti
Laboratory for Welding Process Development – LAPROSOLDA, Federal University of Uberlândia - UFU, Campus Santa Mônica, 38400-902, MG, Brazil, e-mail ascotti@mecanica.ufu.br.

Abstract: *The knowledge of the phenomena that take place in the region close to the work piece is extremely important, since this region (anode region) rules the heat transfer mechanisms from the welding arc to the piece. For instance, once these mechanisms are better understood, proposals for the achievement of a better thermal efficiency can be made. The study of the anode region of atmospheric pressure arcs has been conducted by using the split-anode technique developed in the 1960s. This traditional technique requires a double Abel inversion to reconstruct the local physical information. Thus, in order to reduce (and subsequently eliminate) this mathematical treatment a new modified split-anode detector was designed and constructed. A first version of a detector based on a conductive sheet is presented and the performances of the new set-up are compared under varying arc conditions. Good stability against erratic arcing was obtained using relatively high arc travel speed (60 mm s^{-1}). The signal shape shows a good degree of symmetry in forward and backward motion of the arc through the anode interface, although the disturbance of the latter cannot be avoided completely. The voltage readings obtained at several arc currents fall in between two sets of previously published data.*

Keywords: *plasma current density, split-anode, atmospheric pressure arc and TIG welding.*

1. INTRODUCTION

The knowledge of the phenomena that take place in the region close to the work piece is extremely important, since this region (anode region) rules the heat transfer mechanisms from the welding arc to the piece. For instance, once these mechanisms are better understood, proposals for the achievement of a better thermal efficiency can be made.

Despite extensive use, the well-established optical methods for the characterization of atmospheric-pressure arc columns, in specially TIG arcs, suffer from limited applicability in the anode region (metal vapours, length of measurements, etc). Electrical techniques, while perturbing, can be of great aid in the description of this key region of the arc–material interface. Electrical measurements in arc columns have been performed using Langmuir probes but the minimum distance from the anode plane which allows probe measurements is rarely less than ~0.5 mm (Fanara & Richardson, 2001 and Fanara, 2003). Some authors (Amakawa et al, 1998 and Tanaka & Ushio, 1999) used probes embedded in the anode structure, located at the stagnation point of the arc

jet and protruding from the anode plane a few fractions of a millimetre during a short time interval. The split-anode method has been used in the past (Nestor, 1962 and Schoeck, 1963) to infer both electrical current distribution and heat transfer to the anode ('the work piece'). The principle of the measurement is the following. The anode is cut into two identical blocks separated by a layer of insulating material, typically mica (but even open air has been used) with separation from 0.1 mm upwards. A voltage signal is read while the arc torch crosses the anode, starting when the whole arc is on one side of the block, and ending when the arc has crossed the interface completely at the opposite side (Fig. (1a)). A critical requirement of the set-up is that the thickness of the insulating (or air) interface must be kept to the minimum in order to avoid perturbations of the arc during its crossing. As with Langmuir probes, a major difficulty found in past data interpretation is connected to the inversion of the signals obtained. As these originate from a planar region of variable size, a two-dimensional Abel inversion (Nestor & Olsen, 1960) procedure is required in order to obtain an electrical map of the current density at the anode (radial dependency of the current density).

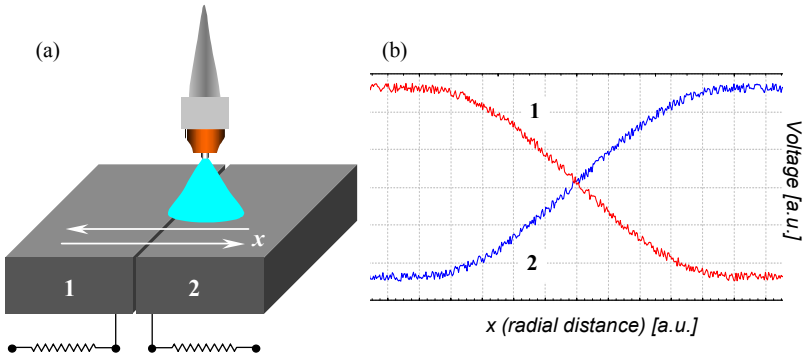

Figure 1. The principle of the split-anode measurement: (a) set-up, (b) qualitative shape of the signals originating in the two blocks.

This double inversion procedure requires double differentiation of experimental data, subject to scatter and experimental error. A major improvement of the method would consist in reducing the dimensionality of the problem in order to use a single Abel inversion procedure or, ideally, to avoid the inversion completely. In the first case, it is possible to obtain a one-dimensional signal by inserting a conducting sheet in between the two blocks, from which it is insulated, and to read the voltage (or current) across a resistor connected to ground. In this case one deals with a linear source as in the case of the electrostatic probes used through the arc column (Fanara, 2003). In common with probes, this arrangement (conductive strip in between the blocks) still shares some difficulties of interpretation. In fact, the question about the correlation between contiguous regions of the conductor, which sum up in the measured signal is still unclear (Fanara, 2003). This calls for a further dimensionality reduction by using an array of vertical wires (instead of the planar sheet) clamped between two thin resistive layers to use their cross-section to act as 'point-like' sensors. In this case one obtains a measured map of the arc at the anode overcoming any inversion problem. This is the subject of an ongoing work.

2. EXPERIMENTAL PROCEDURE

The experimental set-up, including the acquisition circuit, is similar to the one used for probes (Fanara, 2003). Arcs in 5-mm point-plane geometry at currents 50–200 A are struck with argon as shielding gas mass flow at 10 slm (1 slm = 2.97×10^{-5} kg s^{-1}). The TIG arc source is a water-cooled copper block torch. The 3.2 mm tungsten 2% thoriated electrode is ground to a 30º included angle and truncated to a 0.2 mm flat top to prevent erosion, facilitate arcing operation and allow reproducibility. Although relatively complex in geometry, it is believed that the gas flow at the nozzle exit is laminar on the basis of an estimated Reynolds number below 10^{-4}.

The split-anode arrangement is depicted in Fig. (2). It is made of two copper blocks separated by a sandwiched copper strip (Goodfellow, length 120 mm, height 20 mm, thickness 50 μm) insulated with two Kapton® foils (thickness 25 μm). The properties of these materials are reported in Tab. (1).

At one end of the copper foil, emerging from the lateral surface of the blocks, a shielded wire is led to the acquisition system. The floating conditions operation is ensured by a 'high' resistor, R_{DAQ} = 67.72 kΩ (Fig. (3)). The read-out of the signal is performed across a high resistor to ensure floating conditions (zero bias applied) as in a Langmuir probe set-up (Fanara, 2003). The value of the resistor is varied as described in Section 3.

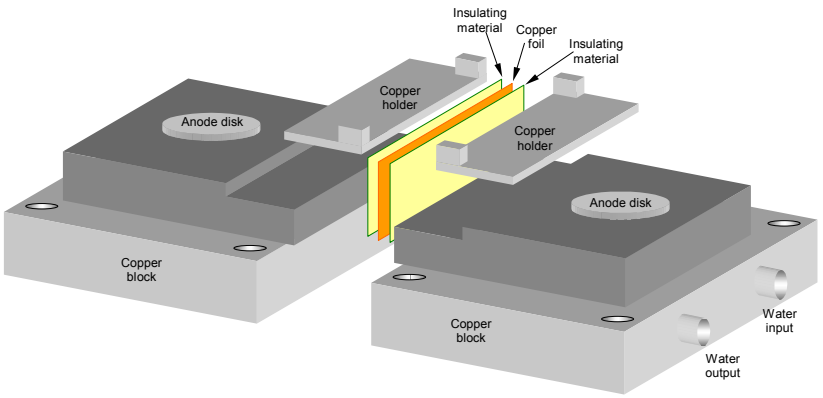

Figure 2. The split-anode set-up.

Table 1. Physical properties of the employed materials (Goodfellow, 2002).

Property	Copper (99.9 %)	Kapton CR®
Electrical resistivity @20ºC [Ω.cm]	$1.69.10^{-6}$	10^{18}
Coefficient of thermal expansion @23ºC [10^{-6} K^{-1}]	17.0	30-60
Thermal conductivity @23ºC [$W.m^{-1}.K^{-1}$]	401	0.10-0.35
Maximum working temperature [ºC]	1083 (melting point)	250-320

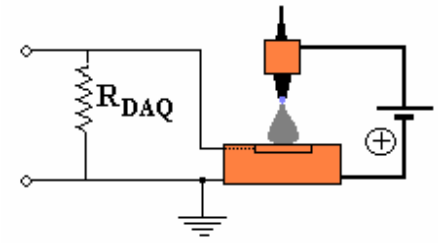

Figure 3. Anode read-out circuits for floating condition.

Because of the high energy transfer to the anode and because of the reduced dimensions of the 'detector' the choice had to be made between moving the torch and therefore the arc, or keeping the arc fixed and moving the whole anode structure. It is well known (Maecker & Stablein, 1986) that an arc in cross-flow will bend and lose its cylindrical shape, which is undesirable in view of the data interpretation. For the arc-bending problem, calculations based on previous work by Maecker & Stablein (1986) show a deviation from the usual bell-shaped structure, which can be quantified using a relationship for the travel speed υ_A and the arc curvature R

$$\upsilon_A = 5\frac{\rho_{\max}}{\rho_{env}}\alpha_{\max}\frac{1}{R} \tag{1}$$

where α_{max} is the maximum thermal diffusivity ($m^2\ s^{-1}$) given by

$$\alpha_{\max} = \frac{k_{\max}}{\rho_{\max} c_{p\max}} \tag{2}$$

where, k_{max} is the thermal conductivity ($Wm^{-1}\ K^{-1}$), ρ_{max} is the maximum density ($kg\ m^{-3}$), ρ_{env} is the environment density ($kg\ m^{-3}$), and $c_{p\ max}$ is the maximum specific heat ($J\ kg^{-1}\ K^{-1}$).

Assuming ambient temperature for the external envelope of the arc, T_{env} = 300 K, the density is ρ_{env} = 1.6224 kg m^{-3}. Using the maximum arc temperatures obtained by spectroscopic measurements (Fanara & Vilarinho, 2002 and Vilarinho, 2002), and the material properties for argon as extracted from Liu (1977) and Murphy (2000), the diffusivity α_{max}, and thus the limiting maximum travel speed υ_A, can be computed once the radius of curvature is known.

For the quantification of the bending, since it is easier to visualize the actual arc bending from its lateral displacement d,

$$d = R - 0.5\sqrt{4R^2 - L^2} \tag{3}$$

where L, the length of the arc, is 5 mm here. The geometry suggests that if one considers a maximum displacement of the order of 10% of the total arc length, i.e., a maximum displacement of 0.5 mm, then the maximum travel speed would be 0.3 to 0.5 m s^{-1} (1.8×10^4 to 3.0×10^4 mm min^{-1}), which is much higher than the ones traditionally applied and ten times higher than the values applied in this work.

This gives a radius of curvature, and the use of Tab. (2) allows the computing of the displacement in terms of the arc current. Some conditions of arc curvature as a function of the travel speed (TS) and the arc current are shown in Fig. (4). Figure (5) shows the bending d occurring in the υ_A range up to 0.18 m s^{-1} for all the currents. At the selected υ_A = 60 mm s^{-1} (0.06 m s^{-1}) the bending lies in between 60 and 110 μm, and thus can be neglected to a first approximation considering the range of arc radii (3–5 mm for the current carrying region, up to 20 mm for the electrical halo (Fanara, 2003)). However, because during the planning and construction of the set-up the optimum speed was not known, it was chosen to move the anode by means of a stepper motor selected by considering the limited space in the chamber and the maximum torque needed to move the complete anode set-up (about 8 kg). This motor (Oriental PK268-E2.0A) provides a torque of 1.35 Nm at 100 rpm. The anode system is capable of linear motion with speed varying from ~3 to 500 mm s^{-1} controlled by four limit-switches mounted on a plane placed adjacent to the slide. A calibration procedure was conducted and the displacement of the anode set-up was determined as a function of the number of steps sent to the motor control unit.

The choice of the anode velocity was critical. On one hand one has to keep the motion as fast as possible in order to avoid damage to the detector and the insulating material during the passage of the arc across the interface. On the other hand, the arc root shows instability around the rectilinear path whilst moving at velocities lower than some tens of mm s^{-1}. After some attempts based on previous work (Nestor, 1962) and observations of ‘walking arcs’ followed by a trail of ‘globular spots’, the value 60 mm s^{-1} was selected in all cases.

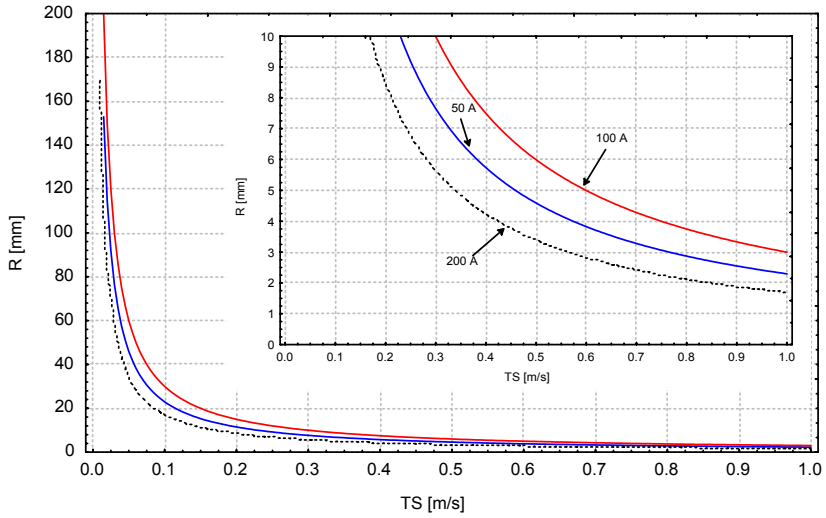

Figure 4. Arc curvature versus travel speed for argon arcs.

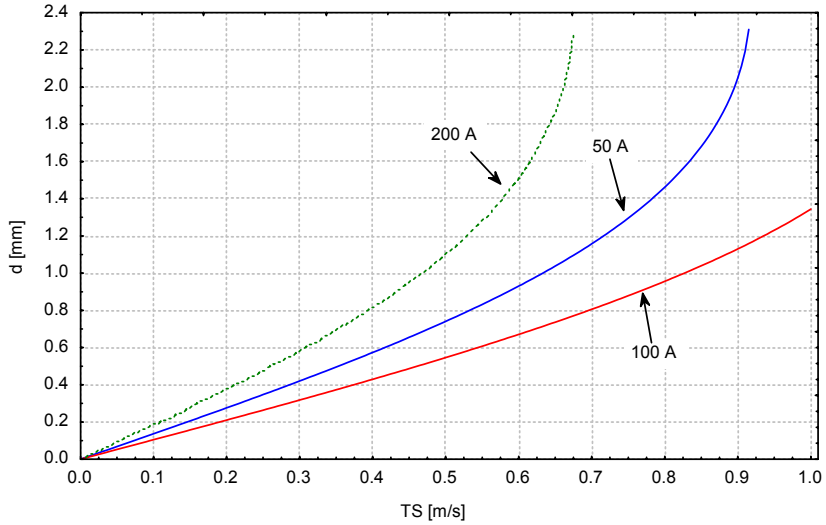

Figure 5. Arc displacement as a function of arc travel speed υ_A for a 5 mm argon arc.

Table 2. Properties as a function of the maximum temperature obtained by emission spectroscopy. The values are taken from Liu (1977) and Murphy (2000).

Current [A]	T_{max} * [K]	k_{max} [W/m·K]	ρ_{max} [kg/m^3]	$c_{p\,max}$ [J/kg-K]
50	18,000	2.3050	$1.4129 \cdot 10^{-02}$	3095.8
100	20,000	2.6666	$1.2318 \cdot 10^{-02}$	2742.1
200	22,000	3.1376	$1.0768 \cdot 10^{-02}$	5708.4

* From spectroscopic investigation (Fanara & Vilarinho, 2002 and Vilarinho, 2002).

After calibration for the anode displacement, both speed and acceleration were evaluated using a circuit, where three micro-switches provide a signal when touched by the tip fixed to the anode blocks. The anode block moves from micro-switch 1 to micro-switch 3, stops and then moves back to micro-switch 1. These movements will be referred to here as forth (1 → 3) and back (3 → 1).

Figure (6) illustrates micro-switch signals for the case for υ_A = 150 mm s^{-1} (1000 steps s^{-1}). A range of 3.75–300 mm s^{-1} was assessed and the results are in agreement with the speed calibration. The acceleration ramp is around 1.4% of the displacement time.

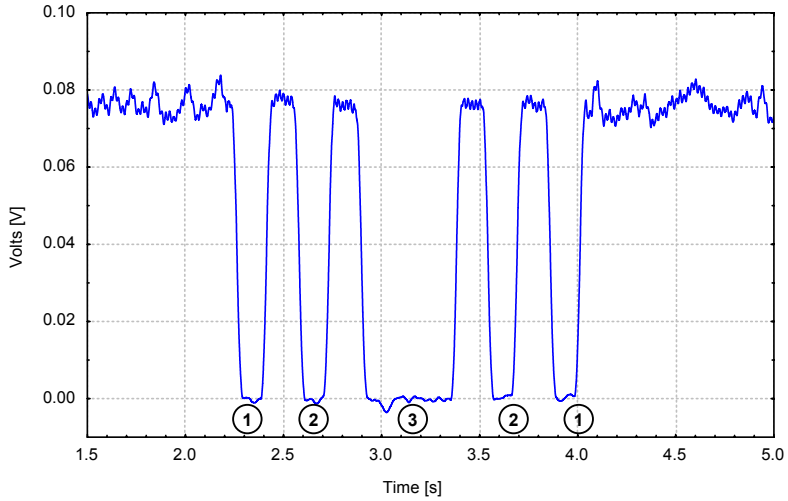

Figure 6. Micro-switch signals for 150 mm s−1 (1000 steps s−1).

3. RESULTS AND DISCUSSION

3.1. Reproducibility and signal symmetry

In order to verify reproducibility and stability and uniformity of arc motion, the anode block was moved back and forth in two subsequent passages of the arc across the interface, providing two experimental signals. Both the calculations of the previous section and the visual inspection of the arc during travel easily rule out any noticeable asymmetry of the arc. Stability and reproducibility of the signals were achieved by the choice of a travel speed of 60 mm s^{-1}. In Figure (7) the traces of the arc paths are shown for (a) 100 mm s^{-1} and (b) the chosen 60 mm s^{-1}.

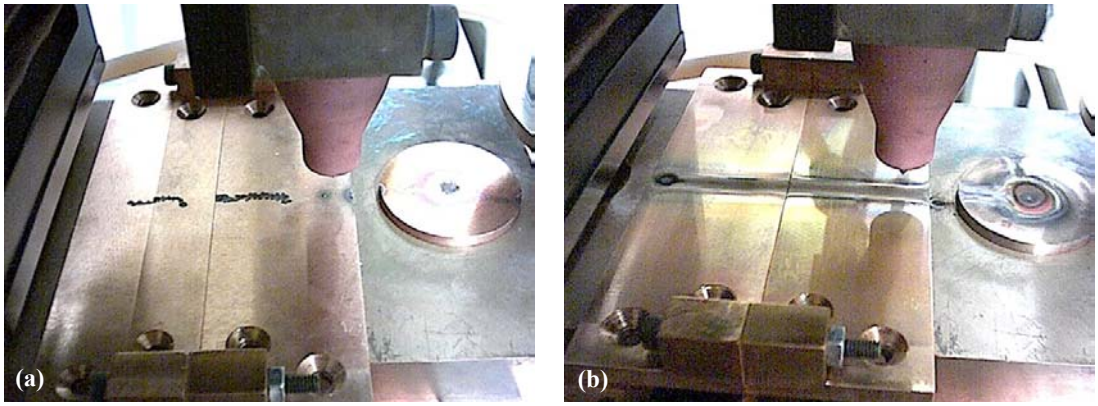

Figure 7. Arc path trace on the copper blocks, 50 A and travel speed (a) 100 mm s^{-1} (b) 60 mm s^{-1}.

Examples of the voltage profiles for forth and back motions are shown in Fig. (8). It can be observed that the two signals show a good degree of symmetry around the central axis and they superimpose satisfactorily. Therefore it is assumed that the bending effects due to arc motion in cross-flow (Maecker & Stablein, 1986) can be neglected, as predicted theoretically in Section 2.

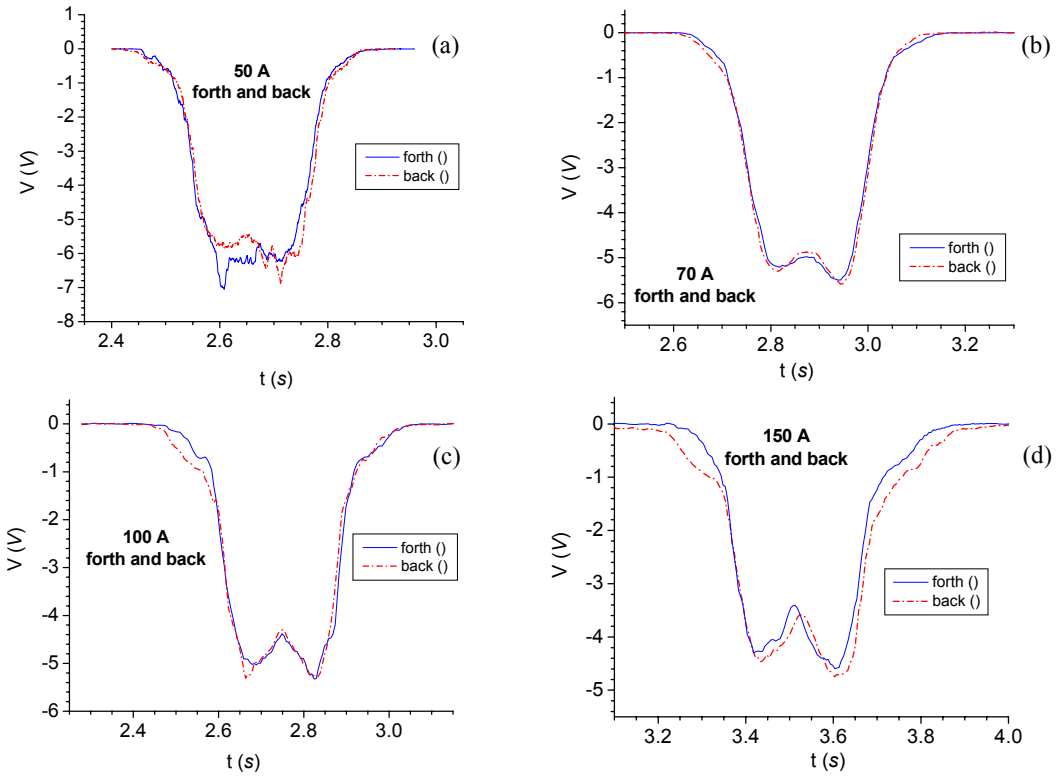

Figure 8. Comparison between forth and back signals obtained for different arc currents.

3.2. Measurements in floating conditions

In Figures (8a–d), a typical signal from the detector operating in floating conditions is shown for the different arc currents 50, 70, 100 and 150 A. The purpose of the tests conducted at various arc currents was to determine the optimum travel speed as a function of the current and to verify signal symmetry. It can be seen from this figure that the voltage fall is higher for lower current, consistent with previously determined arc static characteristic (Fanara & Vilarinho, 2002). For the currents employed here, the highest voltage fall is ~6 V at 50 A. Figure (9) presents the superimposed signals for a better visualisation.

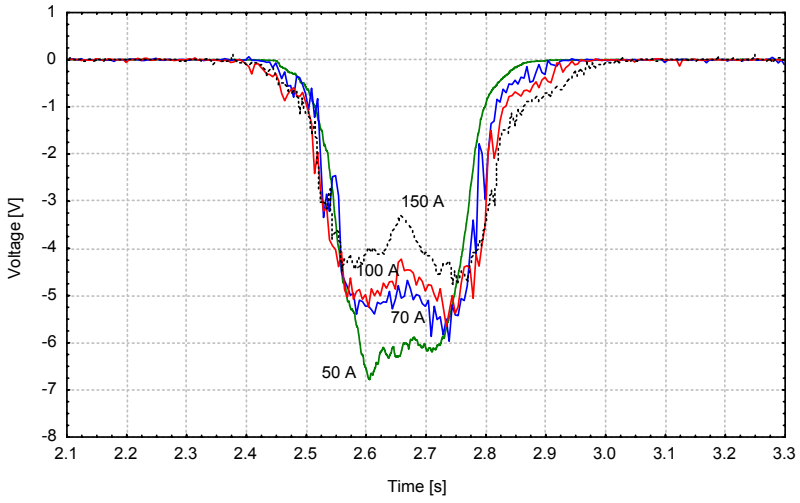

Figure 9. Voltage signal in floating conditions for R_{DAQ} = 67.72 kΩ.

Following the procedure adopted for the Langmuir probe technique, an initial investigation was conducted in order to determine the minimum resistance that should be used in order to obtain the floating conditions. The floating condition for the Langmuir probes is obtained for R_{DAQ} above 15 kΩ (Fanara & Richardson, 2001). Runs at 50, 70, 100 and 150 A arc current were conducted in forth and back movements and the resulting peak heights (central values) are presented as a function of the acquisition resistor R_{DAQ} in Fig. (10) at I = 150 A for voltages in the whole resistor range (a) and in the interval 0–5.7 kΩ (b). An acquisition rate of 20 kHz and υ_A = 60 mm s^{-1} were employed. The values of R_{DAQ} used were 219.2, 67.72, 15.53, 9.942, 4.975, 2.089 kΩ, 994.1, 694.7, 149.6 and 4.2 Ω. The uncertainty for these resistors was 1%. From Figure (10) it is possible to assert that floating conditions are obtained around 67.72 kΩ, where saturation occurs. Thus, this will be the reference value used here for the floating condition analysis. Besides, the voltage fall in the plasma column is small if compared to the cathode and anode falls. Thus, it is possible to assume that the differences in the voltage profiles in Fig. (9) for different currents are due to the voltage fall at the anode sheath. Since it is expected that the lower the current, the larger the sheath and consequently the greater its voltage fall (Schoeck, 1963 and Lukens & Incropera, 1971), the results in Fig. (9) are reasonable.

Moreover, the simultaneous consideration of different arc currents shows a monotonic decrease of the voltage similar to probe floating in the arc column. Figure (11) shows a comparison between the voltage values obtained in this work and the values reported by Schoeck (1963).

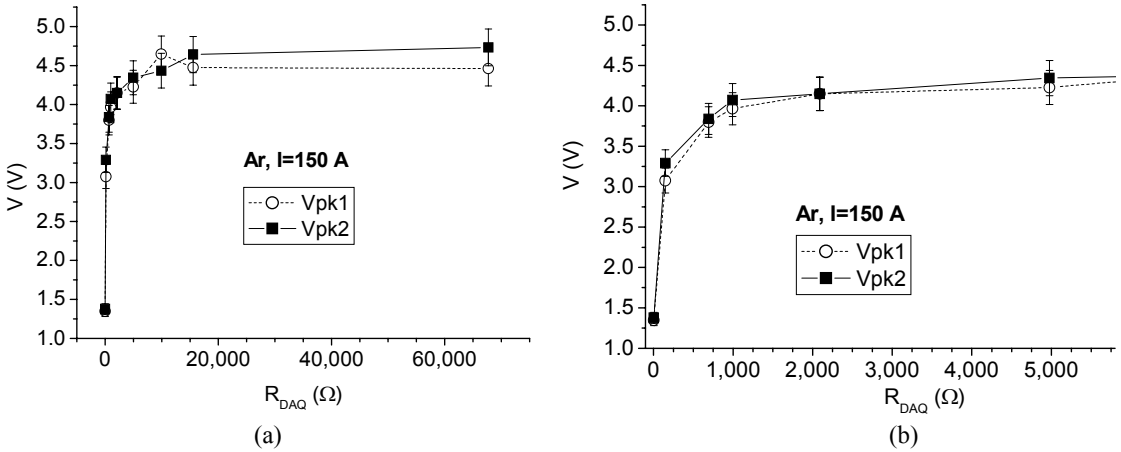

Figure 10. The floating conditions at 150 A strip voltage (a) in the whole resistor range and (b) in a narrow range.

The voltages reported do compare well with Schoeck's computed values. However, the identification of our measured values with those would imply that, in our experimental conditions, the copper foil sheath is 'diluted' in the anode sheath. It cannot be zero, as otherwise a zero voltage would be read, which is not the case. Moreover, by the definition of the floating conditions, the measured voltages for a foil placed at the reference electrode is the foil floating potential, e.g. the potential between the foil and the 'plasma'. In other words, it is only the comparison with Schoeck's values that suggests, in the first instance, that the measured values of this foil floating potential are the values of the anode fall.

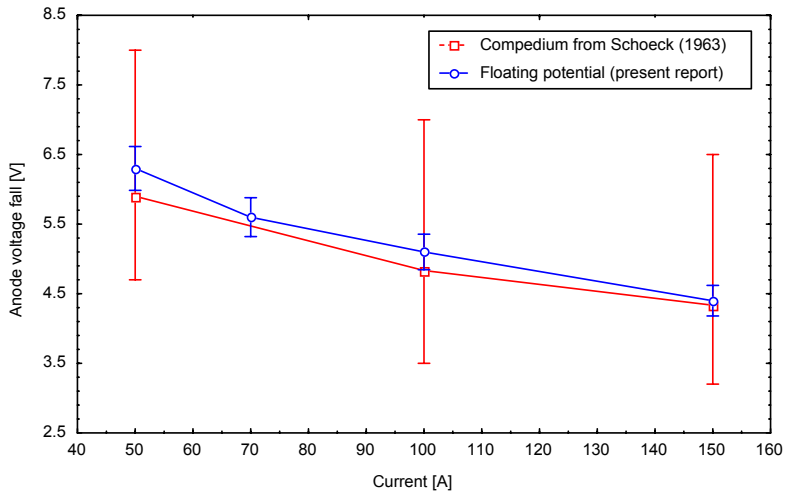

Figure 11. A comparison of voltage falls reported by Schoeck (1963) (full squares) and this work (empty circles) as a function of arc current.

4. CONCLUSIONS AND FURTHER WORK

An upgraded version of the split-anode technique has provided one-dimensional probe-like signals at the anode plane of an atmospheric pressure arc plasma (TIG arc). The arrangement reduces the original two-dimensional (i.e. double) Abel inversion to one. This information can be interpreted in much the same way as Langmuir probes are (Fanara, 2003), bearing in mind that the region investigated is the very peculiar region constituting the lower sheath-edge of the plasma. The combined use of this technique and Langmuir probes will allow us to determine the characteristics of the arc plasma in the anode region and to compare with data reported in literature (Tanaka & Ushio, 1999).

The use of the enhanced multi-wire configuration will eliminate the necessity of any Abel inversion providing point-like signals and, by modifying the read-out system, specifically the electric current density distribution at the location invested by the arc.

6. ACKNOWLEDGMENTS

This work is carried out under EPSRC funded project Grant NB 2648/01 and CAPES project BEX 1148/01-0.

7. REFERENCES

Amakawa, T., Jenista, J., Heberlein, J. and Pfender, E., 1998, “Anode-boundary-layer behaviour in a transferred, high-intensity arc”, J. Phys. D: Appl. Phys., 31, pp. 2826–2834.

Fanara, C, and Vilarinho, L. O., 2002, “Optical and electrical measurements in atmospheric pressure arcs: a comparison”, GEC02: Annual Gaseous Electronics Conf. (Minneapolis, MN, USA, Oct. 2002).

Fanara, C. and Richardson, I. M., 2001, “A Langmuir multi-probe system for the characterization of atmospheric pressure plasmas”, J. Phys. D: Appl. Phys., 34, pp. 2715–25.

Fanara, C., 2003, “A multi-langmuir probe for the characterization of atmospheric pressure plasmas”, PhD Thesis, Cranfield University, 372p.

Liu, C. H., 1977, “Numerical analysis of the anode region of high intensity arcs”, PhD Thesis, University of Minnesota.

Lukens, L .A. and Incropera, F. P., 1971, “Anode heat transfer in a constricted tube arc”, AIAA J., 9 pp. 2453–2454.
Maecker, H. H. and Stablein, H. G., 1986, “What keeps an arc standing in a cross flow?”, IEEE Trans. Plasma Sci., 14, pp. 291–199.
Murphy, A. B., 2000, private communication.
Nestor, O. and Olsen, H. N., 1960, “Numerical methods for reducing line and surface probe data”, SIAM Rev., 2, pp. 200.
Nestor, O., 1962, “Heat intensity and current density distributions at the anode of high current inert gas arcs”, J. Appl. Phys., 33, pp. 1638–1648.
Schoeck, P. A., 1963, “An investigation of the anode energy balance of high intensity arcs in argon”, Modern Developments in Heat Transfer, ed W Ibele, (New York: Academic).
Tanaka, M. and Ushio, M., 1999, “Observations of the anode boundary layer in free-burning argon arcs”, J. Phys. D: Appl. Phys., 32, pp. 906–912.
Vilarinho, L. O., 2002, “Optical emission spectroscopy”, Internal Report (Cranfield: Cranfield University).

8. COPYRIGHTS